PAPER

Tailoring the dissolution rate and *in vitro* cell response of silicon nitride coatings through combinatorial sputtering with chromium and niobium†

Charlotte Skjöldebrand, [ID] ‡[a] Estefanía Echeverri, [ID] ‡[a] Gry Hulsart-Billström[b] and Cecilia Persson [ID] *[a]

Ceramic coatings have been widely investigated as a means to reduce wear and metallic ion release from joint implants. Silicon nitride-based coatings have been a topic of interest specifically due to their solubility in aqueous solutions. This could imply a reduced adverse immune response since the generated debris would dissolve. However, there are concerns regarding the dissolution rate and adhesion of these silicon nitride-based coatings. This study attempts to address the concern of dissolution rate as well as coating adhesion of silicon nitride coatings. We hypothesized that alloying with chromium and niobium would affect the adhesion, dissolution rate, and the resulting ion release and cell response to the coatings. A combinatorial approach was used to deposit sputtered coatings with compositional gradients both with and without a CrN interlayer. Compositional gradients were achieved for all the investigated elements: Si (38.6–46.9 at%), Nb (2.2–4.6 at%) and Cr (1.9–6.0 at%). However, while the presence of an interlayer reduced the delamination during adhesion testing, the differences in composition in the top coating did not affect the adhesion. Nor did the top coating's composition affect the surface roughness or the coatings' inherent mechanical properties (elastic modulus and hardness). All coating compositions were associated with a low Co release from the underlying metal and points with a higher Cr content (4.3–6.0 at%) gave an overall lower release of Si, Cr and Nb ions, possibly due to the formation of a stable oxide, which reduced the dissolution rate of the coating. Optimum chromium contents were furthermore found to give an enhanced *in vitro* fibroblast cell viability. In conclusion, the results indicate a possibility to tailor the ion release rate, which lends promise to further investigations such as tribocorrosive tests towards a future biomedical application.

Introduction

Metals, such as stainless steel, cobalt chromium molybdenum alloys (CoCrMo) and titanium alloys are widely used in orthopedic implants in the form of screws, plates or joint implants. One drawback with using metals is that when placed in the human body they undergo corrosion and subsequent ion release.[1,2] This ion release can escalate further by wear, as seen in the case with metal on metal hip replacements.[3–6] Increased levels of metal ions have been associated with *e.g.*

pseudotumors and clinical implant failure.[7] Therefore, reducing the rate of metallic ion release could be highly beneficial. One strategy for achieving that goal is the use of a ceramic coating deposited on the metallic parts of an implant. The ceramic coating could act as a wear-resistant barrier as well as inhibiting ion release from the underlying metal.

Several material combinations and deposition techniques have been considered for such a coating. Using hip replacements as an example it can be noted that several coated implants have made it to market, *i.e.* titanium nitride coated implants,[8–11] zirconium nitride coated knee implants[12,13] and oxidized zirconium implants.[14–17] While these implants have shown to perform up to par with their uncoated counterparts[14–20] there are still concerns regarding their functionality, the main one being the risk of coating delamination and subsequent accelerated wear.[21,22]

One promising coating material that has not yet reached patients is silicon nitride, a promising material due to low

[a]Division of Biomedical Engineering, Department of Materials Science and Engineering, Uppsala University, Sweden. E-mail: cecilia.persson@angstrom.uu.se
[b]Translational Imaging, Department of Medicinal Chemistry, Uppsala University, Sweden

†Electronic supplementary information (ESI) available. See DOI: https://doi.org/10.1039/d1bm01978c
‡These authors contributed equally.

wear rates,[23,24] reported bacteriostatic properties[25–27] and the possibility to limit adverse effects of wear debris due to its slow dissolution in water, releasing only non-toxic ions.[28–30] Previous studies have found silicon nitride coatings to reduce wear in a hard-on-hard contact[23,24] and metal ion release from the underlying substrate.[31] However, some challenges remain, such as adequate adhesion being challenging to achieve for high-density coatings,[32] and longevity of the coating itself for low-density coatings,[32] *i.e.* a too high dissolution rate that could cause reduced scratch resistance and premature coating failure.[32] Alloying with other elements could allow for tailoring the dissolution rate as well as the adhesion. Further, introducing metallic alloying elements could increase the coating deposition rate. This study investigates the addition of Cr and Nb to silicon nitride coatings. The hypothesis is that alloying the coating with Cr and Nb could improve the adhesion and increase the deposition rate without affecting important properties such as hardness. Nb has previously been used to alloy TiN coatings, as a biocompatible element[33,34] and Cr is already present in the underlying CoCrMo alloy, most commonly used in the bearing part of the hip implant.[35] Indeed, Cr is a key element in many corrosion-resistant alloys due to its capability for forming a passivating oxide, a property that could be of benefit also here. Therefore, this study aimed to investigate the possibility of Cr and Nb as alloying elements in SiN coatings with and without CrN interlayers to tailor the ion release and adhesion while maintaining surface and mechanical properties, as well as biocompatibility.

Materials and methods

Coating deposition

The SiCrNbN coatings were deposited in two batches on both Si wafer and cobalt chromium molybdenum (CoCrMo, Peter Brehm) disc substrates by reactive sputtering (Fig. 1) in a set-up built in-house.[36] The base pressure in the chamber prior to deposition was ≤10^{-8} Torr and during deposition the pressure was kept at 3×10^{-3} Torr. The sputtering gas used was Ar, which was introduced at the individual targets and the reactive gas, N, was supplied at the substrate. The gas flow was 10.000 sccm for Ar and 3.000 sccm for N, resulting in a N to Ar ratio of 0.3. The solid targets (3 inch or 76.2 mm in diameter), Si (99.99% purity), Cr (99.99% purity) and Nb (99.99% purity), were individually powered with a pulsed DC aggregate for Si (150 W, 100 kHz and 4 μs pause time) and DC for Cr (10 W) and Nb (20 W) for the first batch. The second batch had identical deposition parameters apart from the target bias and pause time for Si (200 W and 2 μs). In addition, the targets were placed at 175 mm distance and an angle of 45° making it possible to achieve compositional gradients. The deposition time was 10 000 s and the substrate temperature were kept at 250 °C throughout. Reference SiN coatings were made with the same parameters but without the use of Cr and Nb targets.

Prior to deposition the substrates were cleaned ultrasonically in 70% ethanol for 10 min and heated *in situ* for 20 min at 250 °C.
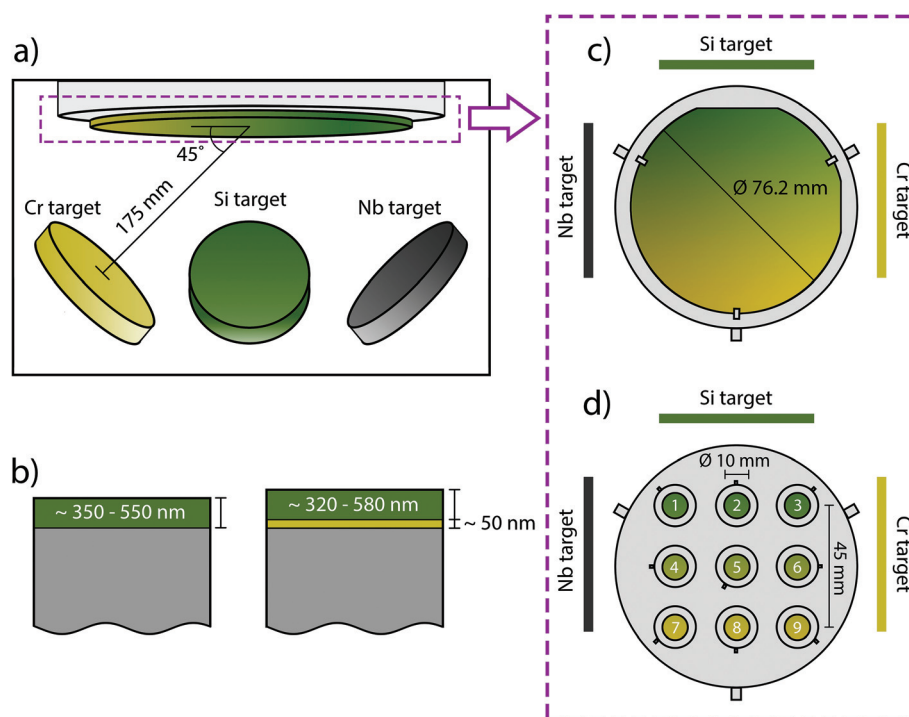

Fig. 1 A schematic view of the deposition chamber and target placements (a), the two types of coatings, with and without interlayer are illustrated (b). As well as the two different substrate types used, namely Si wafers (c) and CoCrMo discs (d). To illustrate the expected gradients the positions of the targets during deposition are indicated, as well as the numbering of the CoCrMo substrates (d).

Two sample holders were used depending on the substrate, one for Si-wafer and one for CoCrMo discs (Fig. 1(c) and (d)). The former samples were used to determine composition. The latter were used during nanoindentation, Rockwell indentation, surface roughness and appearance, dissolution and *in vitro* studies.

The parameters used for the first round (100 kHz and 4 µs) were found to cause arcing. This resulted in two batches (batch 1 and batch 2) and for batch 1 coatings were deposited both with and without interlayer while for batch 2 all coatings had a CrN interlayer.

Material characterization

Composition. The composition was examined with X-ray photoelectron spectroscopy (XPS) with a monochromatic Al source (Quantera II, Physical Electronics, USA). Measurements were performed with an X-ray power of 100 W and a spot size of 100 µm, after 3 min (batch 2) or 20 min (batch 1) of sputtering with Ar$^+$ ions at 200 V.

Surface properties. The surface roughness was investigated using vertical scanning interferometry (VSI, NexView, ZYGO, Berwin, PA, USA). VSI was used over an area of 1×1 mm comprised of 16 individual measurements with a 50× objective, 0.5 zoom and scan length of 10 µm. A spherical form removal was applied before calculating the surface parameters average surface roughness S_a, root mean square roughness S_q and maximum height S_z according to ISO 4287.

The surface appearance was investigated with scanning electron microscopy (SEM, Merlin, Zeiss, Germany) with an acceleration voltage of 1 kV and probe current of 80 pA. The samples were investigated again post dissolution with the same parameters. In addition, energy dispersive X-ray spectroscopy (EDS, Merlin, Zeiss, Germany) was performed at 10 kV and 200 pA.

Hardness and elastic modulus. Hardness (H) and indentation modulus (M) of the coatings were determined by nanoindentation (UNHT, Anton Paar, Graz, Austria). The measurements were conducted with a modified Berkovich tip to a depth of 50 nm, and 25 indents were made on each sample. The measurements were repeated on three different samples. The indentation modulus relates to Young's modulus (E) as $E = M(1 - \nu_s^2)$,[37] where E is Young's modulus, M the indentation modulus and ν_S Poison's ratio of the sample.

Adhesion. Due to the gradient nature of the coatings, the method used to evaluate adhesion was Rockwell indentation (as opposed to *e.g.* scratch testing), according to ISO 26443.[38] A Rockwell C tip (diamond tip with 200 µm tip radius and 120° apex angle) was indented with a load of 100 kgf, and the resulting indent was imaged in a light optical microscope (AX70 Research Microscope, Olympus, Tokyo, Japan) and graded 0–3 according to ISO 26443. A grade of 0 means no cracking nor delamination, 1 is cracking without adhesive delamination, 2 is partial adhesive delamination with or without cracking and 3 is complete adhesive delamination.

Dissolution behaviour. The dissolution behaviour was evaluated by exposing the materials to DMEM cell culture media

with 1% penicillin/streptomycin and incubation at 37 °C, 5% CO$_2$ for 14 days. The dissolution was done without the addition of FBS to avoid contamination and to enhance the extraction of ionic compounds. The container used had wells with a diameter of 8 mm, with viton O-rings at the edge to prevent leakage. This resulted in a specimen surface area-to-cell culture medium volume ratio of 0.47 cm^2 mL^{-1}. Before the dissolution, the container was autoclaved and the sample sterilized by immersion in 70% isopropanol for 10 minutes. At the end of the dissolution period, the samples were rinsed under deionized water followed by sonication for 10 min in deionized water, 10 min in 0.02% (v/v) detergent and 10 min in 70% (v/v) ethanol. In between each sonication the samples were rinsed in deionized water. The extracts were collected into sterile tubes and stored at −20 °C until used for ion release analysis with inductively coupled plasma atomic emission spectroscopy (ICP-OES) and for indirect *in vitro* cytotoxicity tests.

The concentration of Cr, Nb, Co and Si ions in the extracts was analyzed by ICP-OES (PekinElmer ICP-OES, Avio 200). Before the measurement all the test solutions were acidified to a 2% HNO$_3$ concentration for matching the matrix with the one of the standard solutions used and avoiding interference from physical properties (*e.g.* viscosity) on the measurements. For each analysis the instrument performed three measurements and calculated the mean and relative standard deviation (SD) for each element. The measurements were done using extracts obtained from coatings with an interlayer (batch 2). All handling of the extracts was done with plastic utensils and no glassware to avoid Si contamination.

Indirect cytotoxicity measurements. Mouse fibroblast cells L929 (ECACC No. 85011425) were cultured in Dulbecco modified eagle medium (DMEM) (Gibco 11965092) supplemented with 10% fetal bovine serum (FBS) (Gibco 11560636) and 1% penicillin/streptomycin (Sigma-Aldrich P433). Cells were incubated at 37 °C in a 5% CO$_2$ incubator and passaged upon reaching 70% confluency every 2–3 days.

The cytotoxicity of the coated samples, SiN, and CoCrMo controls was evaluated by testing leach extracts from the dissolution tests using the tetrazolium dye MTT. L929 cells were seeded in 96 well plates, at a cell density of 3200 cells per well (10 000 cells per cm^2). After 24 hours, the medium in each well was replaced with 100 µL of extracts (0% FBS) and 100 µL of cell culture medium with 20% FBS to a final concentration of 10% FBS. The obtained extracts were diluted to different extents (undiluted extracts (1:1), 1:8, 1:12 and 1:16 dilution) to evaluate potential differences between compositional points on the coating surface. The cell viability was assessed on days 1, 2 and 3 after the cells were exposed to the extracts. Each extract dilution was applied to L929 cells with triplicate wells for each time point. Culture media served as negative control, and DMSO served as positive control. The absorbance of each extract was normalized to the absorbance of the negative control. Data are presented as the mean ± standard deviation of at least three independent experimental replicates. The experiments were carried out using coatings with an interlayer (batch 2). Extracts causing a decrease in viability below 70%
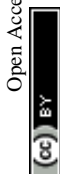
were considered cytotoxic. The experiments were repeated three times.

Statistical analysis

The statistical analysis was performed using IBM SPSS Statistics for Windows, version 28 (IBM Corp., Armonk, N.Y., USA). Pearson correlation coefficients were computed to assess any correlations between coating composition and ion release. Cell studies were analyzed using one-way ANOVA and differences between groups were determined with Dunnett's *post hoc* analysis. A *p* value <0.05 was considered indicative of statistical significance.

Results

Coating composition

The compositional analysis revealed gradients of Si ranging from 38.6–46.9 at%, Cr 1.9–6.0 at%, Nb 2.2–5.5 at%, N 40.5–42.6 at% and O 5.5–11.4 at%, the compositions being similar for coatings with and without interlayer. The gradients

(Fig. 2) exhibit the expected trends from the placement of the targets during deposition.

Adhesion, hardness and elastic modulus

The use of interlayers was deemed necessary, which was supported by the Rockwell indentation results, which revealed ISO grades from 2 to 3 (ISO 26443) for coatings without interlayer and 0 to 2 (ISO 26443) for coatings with interlayers (Fig. 3). There was hence a noticeable improvement for coatings with an interlayer, from an average of ISO 2 with 24.2% delamination without interlayer to an average of ISO 2 with a delamination of 1.6% and two cases of ISO 0 (point 6 and 7) with interlayers, which was necessary for conducting other evaluations.

The presence of an interlayer did not affect hardness, indentation modulus or the surface roughness (see the next sections). However, the use of an interlayer was found to be necessary when conducting investigations into dissolution and subsequently cytotoxicity due to the risk of delamination. Hence, only coatings with interlayers were used for these investigations.

As the adhesion is of the utmost importance the further investigations were only performed on samples with interlayer,
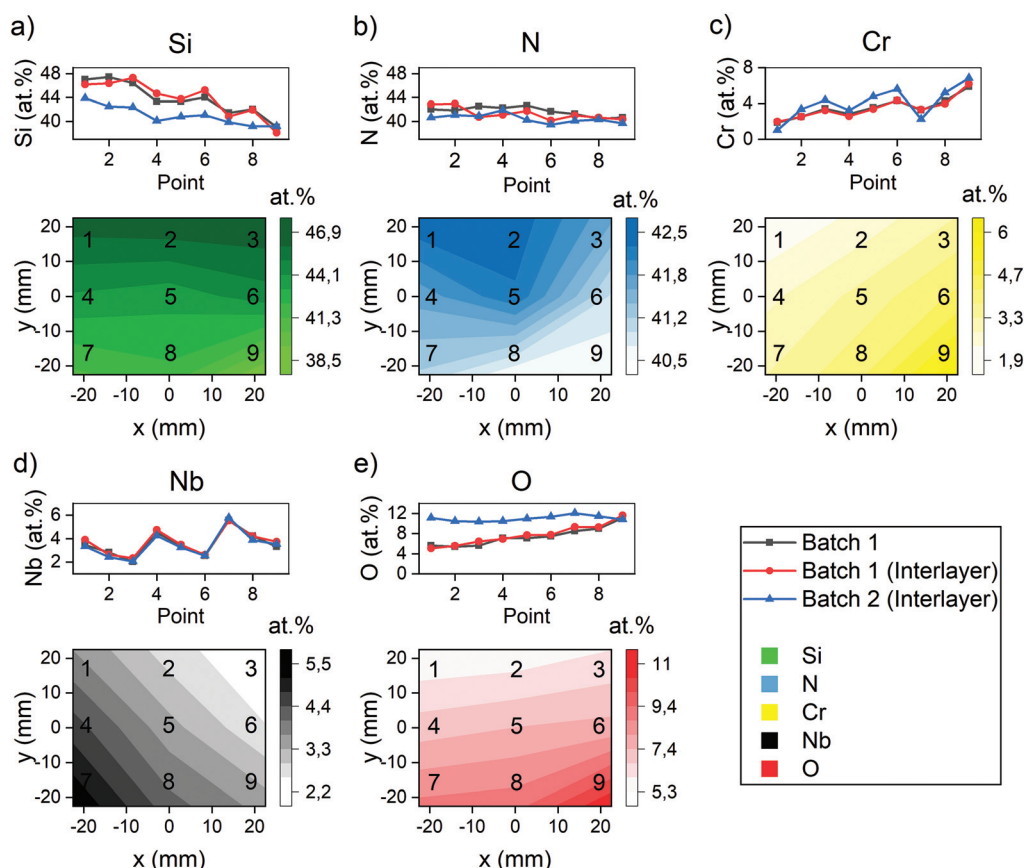

Fig. 2 The composition as measured with XPS. The measurements are conducted in each point, and the gradients have been calculated using a piecewise linear interpolation in between 3 neighbour points. The points refer to the sample positions during deposition, see Fig. 1. The Si concentration (a) exhibits a gradient that is higher in points 1, 2 and 3 compared to the other points, which is expected considering the placement of the target. The N concentration (b) also exhibits a gradient despite being supplied as a gas. Similarly to the Si concentration, the Cr concentration (c) and Nb concentration (d) behave as expected when considering the target placements. The O concentration (e) correlated to the Cr concentration.
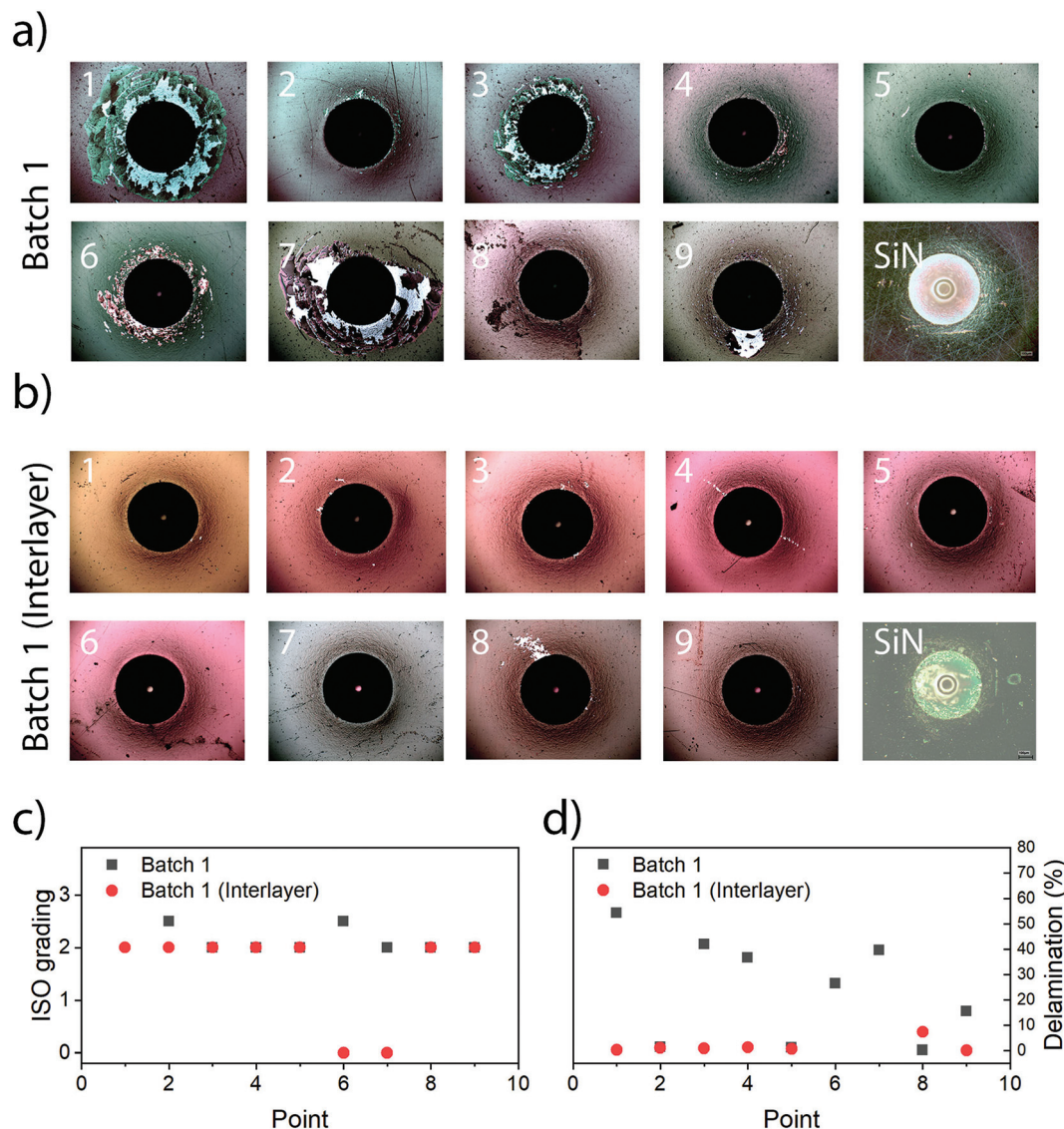
Fig. 3 Adhesion as evaluated by Rockwell indentation. The indents are depicted for SiCrNbN without interlayer (a) and with interlayer (b) for all points (1–9) and the SiN reference. The ISO grading as a function of the Si content (c) reveals no major differences until the delamination for ISO 2 is examined closer (d). Coatings without an interlayer show more delamination than those with.

i.e. showing a satisfactory adhesion. Hardness and modulus ranged from 11.0 to 12.4 GPa and 190 to 198 GPa (Fig. 4), respectively, with no significant difference between points. This can be compared to 9.9 ± 1.2 GPa and 267 ± 25 GPa for the uncoated CoCrMo substrate.

Surface roughness

The investigated surface roughness parameters revealed no significant difference between points (Fig. 5). The average surface roughness, S_a, from 4.8 ± 1.1 nm to 7.1 ± 1.0 nm for SiCrNbN in combination with a CrN interlayer for batch 1 and from 6.7 ± 2.2 nm to 9.4 ± 1.1 nm for the SiCrNbN coating with interlayer from batch 2. The root mean square roughness, S_q, values ranged from 8.5 ± 2.1 nm to 26.8 ± 13.9 nm for coatings with interlayer from batch 1 and 9.7 ± 0.9 nm to 14.5 ± 2.8 nm

for coatings with interlayer from batch 2. The maximum height, S_z, ranged from 1480 ± 630 nm for the coating with an interlayer for batch 1 and from 370 ± 118 nm to 980 ± 386 nm for batch 2 with interlayer. This can be compared to uncoated CoCrMo with a S_a of 4.2 ± 1.1 nm, S_q 14.8 ± 15.0 nm of and S_z of 430 ± 220 nm for batch 1 and S_a of 7.9 ± 1.1 nm, S_q 11.0 ± 1.75 nm of and S_z of 412 ± 184 nm for batch 2.

The surface morphology was also investigated in SEM (Fig. 6) and in these images the scratches from polishing the substrate are still visible, as well as the coating surface texture.

Dissolution behaviour

The ion concentration in the extracts showed that the level of Co (Fig. 7(a)), that is only present in the substrate, was around 17 times lower for all coated samples compared to the
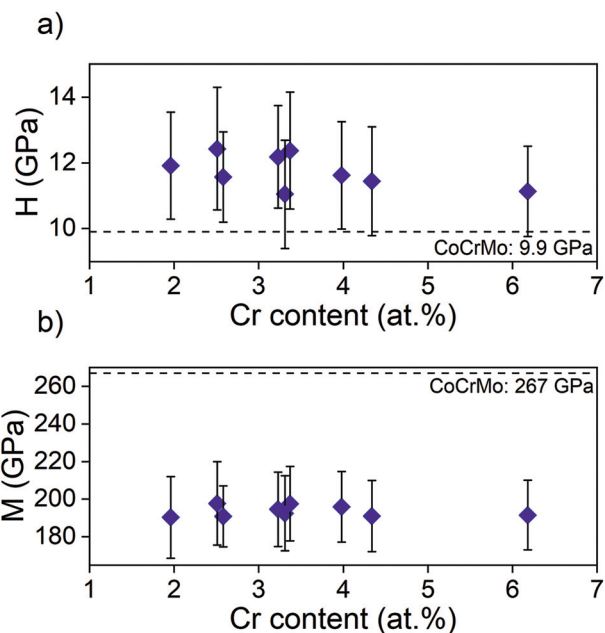
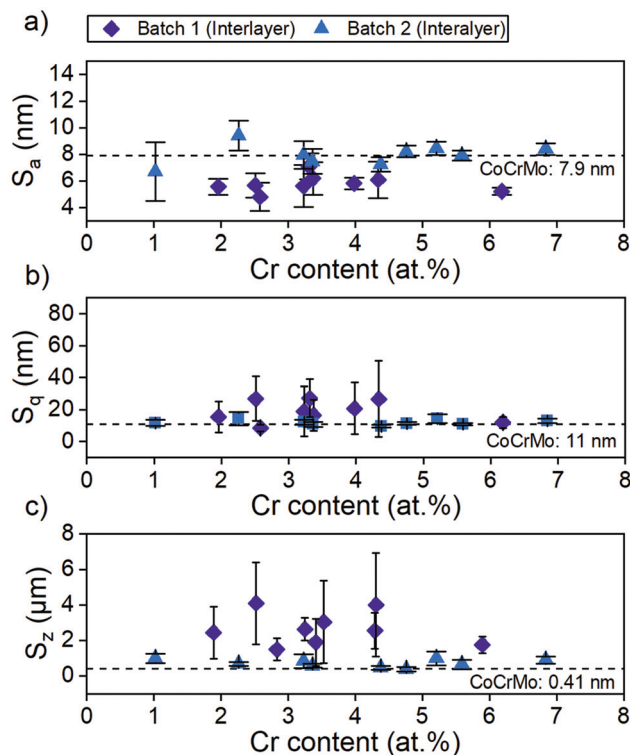**Fig. 4** (a) Hardness, H, and (b) elastic modulus, M, obtained using nanoindentation on samples from batch 1.

Fig. 5 Surface roughness obtained with VSI. The investigated parameters S_a (a). S_q (b) and S_z (c) are presented as individual graphs containing data for coating with interlayers from both batch 1 and 2.

uncoated CoCrMo reference. The levels of silicon released from the coatings with alloying elements were around 6 times lower than the SiN reference coating. For the alloyed coatings,

the most apparent trend was that the detected levels of Si, Cr and Nb (Fig. 7(b)–(d)) were lower in the points with a higher Cr content in the coating, indicating a positive effect of the Cr content on the dissolution rate. This was further confirmed by looking into trends of Nb and Si release (ESI Fig. S2†) – the highest release of Si was found for the point 1 with the highest amounts of silicon and lowest amount of Cr, and the highest release of Nb was found for the points 1, 2 and 4, which contained varying amounts of Nb (but not the highest) and the lowest amounts of Cr. The point with the highest amount of Nb (point 7) gave a higher Nb release than some of the other points, but not higher than the points with a lower Cr content. Statistical analysis revealed that the Cr content of the coating had a statistically significant ($p < 0.01$) negative correlation to the Nb (r: −0.825), Cr (r: −0.752) and Si (r: −0.733) ion release. Also, the Si content of the coating had a statistically significant ($p < 0.01$) positive correlation to the Nb (r: 0.5899), Cr (r: 0.780) and Si (r: 0.7778) ion release.

The samples were observed in the SEM after dissolution and this revealed changes in the surface morphology (Fig. 8). After dissolution the surface appeared more porous and this was more noticeable for points 1, 4 and 7, *i.e.* the ones with lower amounts of Cr, again confirming the previous findings. In addition, point 2 exhibited an appearance similar to point 4, which can be explained by the Cr content which is 3.36 at%, only slightly higher than 3.23 at% in point 4.

Additionally, EDS was performed at the edge of the wells (Fig. 9). These measurements revealed a higher oxygen content inside of the wells implying a change in composition of the surface for the material exposed to cell medium. The higher oxygen content in the exposed area compared to the un-dissolved coating supports the formation of a surface oxide during dissolution. However, the extent of the coverage of this oxide could not be determined, due to the lack of precision of the EDS technique.

Indirect cytotoxicity

In a preliminary cytotoxicity study undiluted extracts (1 : 1), as well as 1 : 2, 1 : 4, 1 : 8, 1 : 10, 1 : 12, 1 : 16 and 1 : 32 dilutions were evaluated. There, the cell viability remained higher than 70% for the 3 days for all the coated samples only after 16 times dilution. The 16 times dilution was therefore chosen to compare the samples as it showed differences between samples while maintaining high enough levels of cell viability (see the ESI, Fig. S2†).

Fig. 10 shows the cell viability for the 9 coated sample points and the CoCrMo and SiN controls at 16 times dilution. All samples showed a significant difference ($p < 0.05$) with the DMSO positive control on day 1, however on day 3 the samples with Cr content higher than 5.21 at% showed a decrease in viability comparable with the positive control. In addition, coatings with Cr content lower than 3.36 at% also showed a reduction in cell viability. Extracts from the coated samples alloyed with Cr and Nb showed a higher viability than the extracts from CoCrMo and SiN controls. From the different coated samples the points that had a Cr content between 3.36
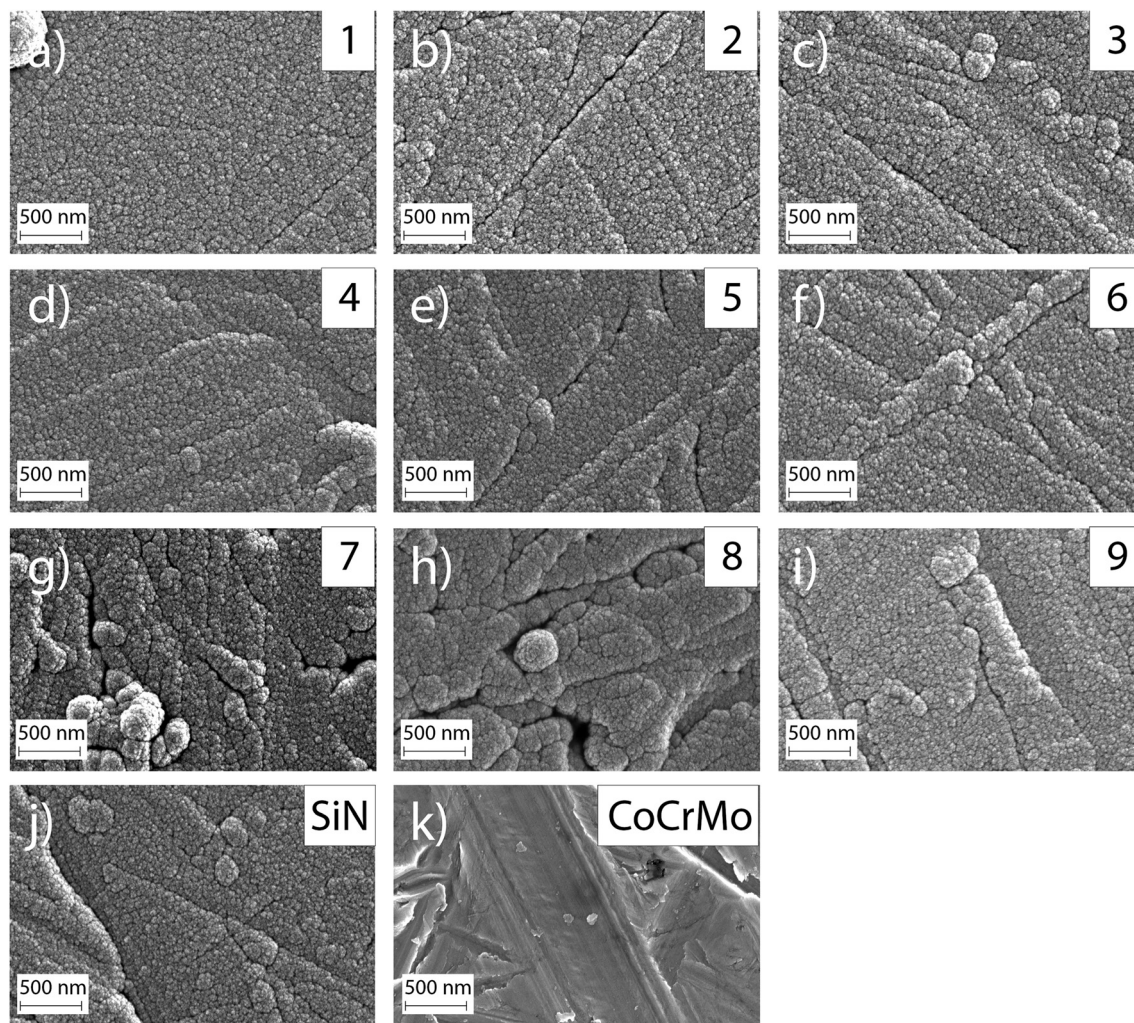
Fig. 6 SEM images of coated samples 1–9 (a)–(i) revealing a surface with still visible scratches from polishing and a textured surface. The reference coating SiN (j) exhibit a similar apperence and (k) shows an uncoated CoCrMo sample.

at% and 5.21 at% (points 2, 3, 5 and 8) presented values greater than 70% for the 3 time points, where point 2 (3.36 at%) in particular showed viability values closer to 100% and an increase in viability over time after a small decrease on day 1. The points with the highest Cr content (6 and 9) gave the lowest viability.

Discussion

In this study, SiCrNbN coatings of different compositions, with and without CrN interlayers, were successfully deposited using a combinatorial approach. As the intended application of these coatings are medical implants it was of interest to investigate properties known to limit implant lifespan or affect the implant functionality. One of the most prominent properties limiting metallic implants is the release of metal ions, causing a negative biological response, in some cases leading to revision surgery. Similarly, a main concern of coated

implants is the dissolution rate of the coating itself as well as the risk of delamination. Hence, the focus of this study has been to tailor the ion release and adhesion while leaving properties such as surface roughness, hardness and elastic modulus unaffected.

The use of interlayers improve the adhesion, as expected.[39–43] The Rockwell indentations revealed ISO grades from 0 to 2 [38] but the delamination was decreased for coatings with a CrN interlayer. A study by Filho *et al.* that investigated the adhesion using Rockwell indentation found similar results for a SiN_x coating, with an improvement from an ISO grade of 3 to a grade 0–2 when employing CrN interlayers.[32] The use of CrN interlayers does seem to reduce the risk of delamination to acceptable levels and could be used also for these coatings.

The combinatorial approach resulted in compositional gradients of 27.4 at% < Si < 32.8 at%, 4.1 at% < Cr < 10.9 at% and 3.5 at% < Nb < 8.4 at%. These gradients were to be expected because of the placement of the targets during deposition. There was also a N gradient that correlated with the Si gradi-
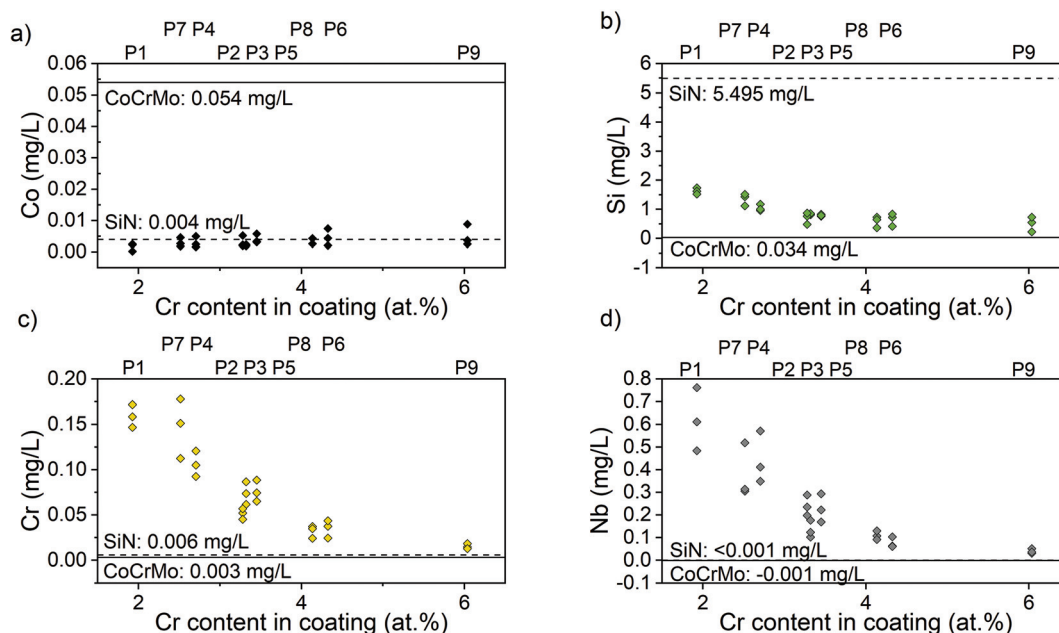
Fig. 7 Ion concentration from the 9 points on the samples surface. (a) Co ions; (b) Si ions; (c) Cr ions; (d) Nb ions. The corresponding release from CoCrMo and SiN references is indicated as lines in each graph. The point number corresponding to the Cr content is indicated above each graph.

ent, likely because of the high affinity of silicon to nitrogen. The oxygen content ranged from 11.0 at% to 14.6 at%, which is similar to what was found in a study by Filho *et al.*[32] for SiN coatings with a lower density. The O content was attributed to the coating porosity that intensified the C and O content upon exposure to air. Low target power and substrate temperature was likely to yield a higher porosity and could therefore explain the O content. The difference in deposition parameters between batch 1 and batch 2 herein was the target bias and pause time of the Si target (150 V, 100 kHz and 4 μs compared to 200 V, 200 kHz and 2 μs). A higher degree of ionization of the plasma and subsequent energetic bombardment could result in more compressive stresses in the coating.[44] This could in turn yield a higher coating density,[45] however also adhesive failure. The difference in oxygen content between batches could be due to a higher oxygen contamination during deposition. It is also possible that it is a consequence of the differences in sputtering time prior to measurement (3 min compared to 20 min at 200 V). After 3 minutes the oxygen content could still be higher while after 20 minutes the composition could be constant through the film. A depth profile of SiCrNbN coating in point 5 deposited on a Si wafer (ESI, Fig. S1†) showed a surface oxide that was removed after approximately 180 s of sputtering.

A property known to exacerbate ion release is wear. However, due to the compositional gradients it is difficult to perform investigations into wear properties at this stage. Tribological tests to investigate the wear properties would cover an area, which on these samples would mean a range of compositions. Therefore, this study focused on parameters that could indicate a positive future wear performance such as

surface roughness, adhesion and the ratio of H/E. Both the hardness and elastic modulus were comparable to similar coatings found in literature[23,24,46,47] and no effect from either composition or interlayer could be observed. Another property not affected by the composition was the surface, which remained smooth after coating deposition. A low surface roughness is necessary for medical implants exposed to wear such as joint implants and S_a values of 50 nm has been specified in the ISO standard 7206-2.[48] The roughness of these coatings is well within the acceptable range, however the coatings in the final application will likely be thicker and a longer deposition time can influence the roughness. The results for these coatings show an S_a ranging from 7.3 ± 2.6 nm to 9.3 ± 4.5 nm for the SiCrNbN coating and from 4.8 ± 1.1 nm to 7.1 ± 1.0 nm for SiCrNbN with a CrN interlayer, which is a minor increase compared to the uncoated CoCrMo (4.2 ± 1.1 nm). There is however an increase in S_z compared to uncoated substrates. This is likely due to coating defects formed during deposition due to *e.g.* arcing.[49] Batch 2 had lower S_z which is likely related to less arcing and subsequent surface damages. A lower frequency with a longer pause time resulted in the Si targets experiencing arcing and for the second batch the frequency was increased to 200 kHz and the subsequent pause time was 2 μs. This is in accordance to what has previously been observed for insulators such as Al_2O_3.[50,51]

All coatings showed reduced levels of Co ions in the extract, indicative of the ability of SiN to protect the surrounding environment from ion release from the substrate. There was no discernible difference between different compositions. Similar results were found by Pettersson *et al.* who found a decrease in released Co ions for CoCrMo samples coated with
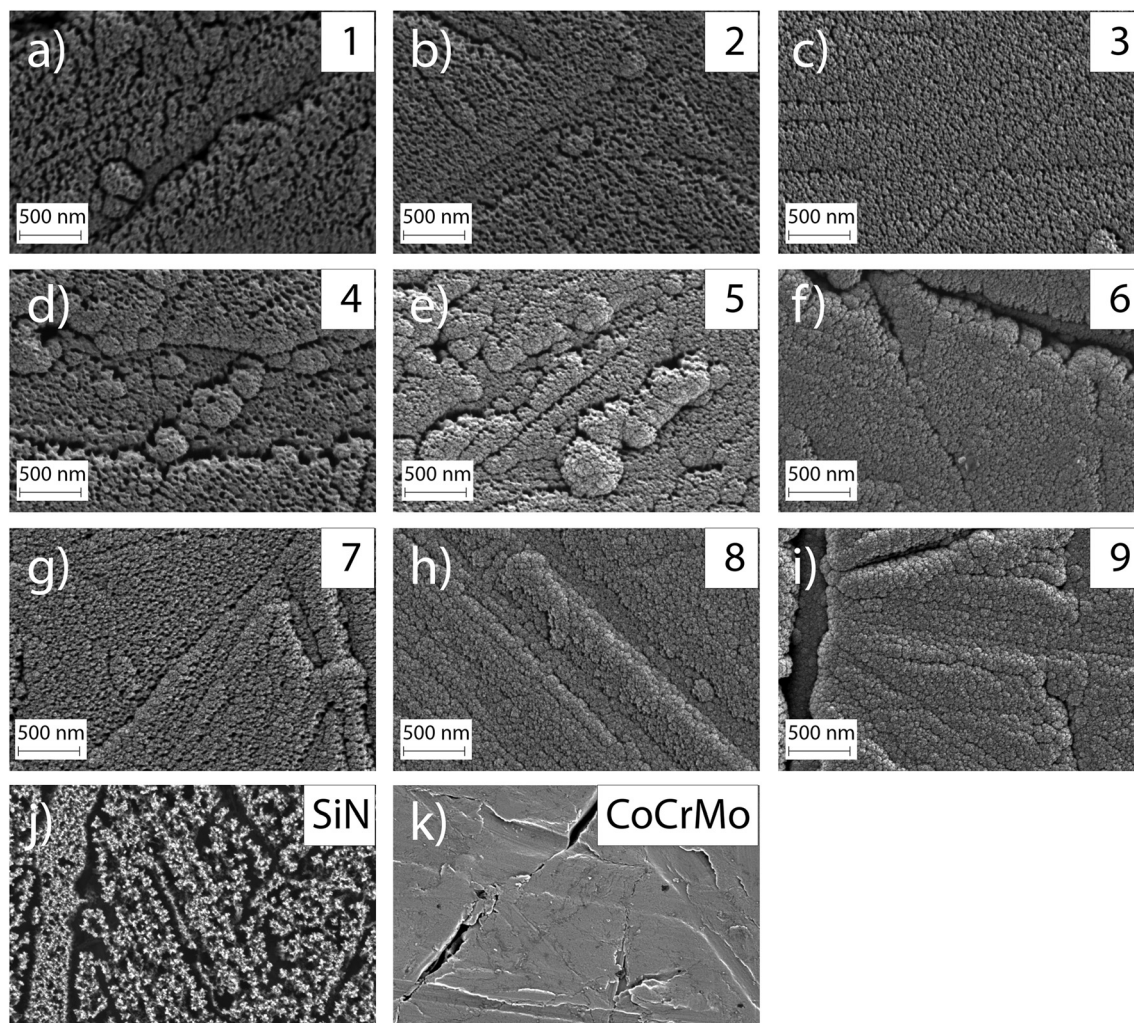
Fig. 8 SEM images of the surfaces of points 1–9 (a)–(i) after dissolution in DMEM cell culture media for 14 days. The surface texture has changed and the appearance is more porous for samples 1, 2, 3, 4, 5 and 7. The SiN reference coating (j) appears to have a more severely affected surface and the CoCrMo reference is shown as comparison (k).

SiN compared to uncoated references.[31] Previous studies have however not looked into the release from the coating itself. In this study, the levels of Si detected were lower for the coatings with Cr and Nb as alloying elements compared to the SiN reference coating. The concentration of Si measured in the extract from SiN coating was 5.6 mg L^{-1}. Fu *et al.* conducted some studies including the ion release from SiN bulk materials (with 0.25 cm^2 ml^{-1} surface area to volume ratio), and found a Si ion release after 24 h that fluctuated from 0.02 mg L^{-1} to 22 mg L^{-1} depending on the sintering elements and the immersion medium chosen for the dissolution (milliQ water, DPBS or cell culture medium).[52,53] A direct comparison is difficult because of the differences in extraction time, immersion medium and specimen surface area to volume ratio between the studies.[54,55] However, the results showed that the coatings can dissolve but that the addition of Cr and Nb reduces the dissolution rate, which is beneficial for the integrity and longevity of the coatings.[56,57]

In particular, this study showed that the Si content of the coating had a statistically significantly correlation with the Nb, Cr and Si ion release. This was expected since Si is the predominant element in the coatings. Furthermore, the results revealed an overall reduction of ion release for coatings with higher at.% Cr in the coating itself. Statistical analysis revealed that the chromium Cr content of the coating was significantly negatively correlated with the Nb, Cr and Si ion release. This is believed to be caused by the formation of a stable oxide that reduces the dissolution rate. The oxide formed is likely to contain a high fraction of Cr and Nb as can be assumed by looking at the enthalpy of formation. The enthalpy of formation for Cr$_2$O$_3$ is −1139.7 kJ mol^{-1} and −1531.0 kJ mol^{-1} for Cr$_3$O$_4$, for Nb based oxides it is −405.8 kJ mol^{-1} for NbO, −796.2 kJ mol^{-1} for NbO$_2$ and −1899.5 kJ mol^{-1} for Nb$_2$O$_5$, while other oxides such as SiO has an enthalpy of formation of −910.7 kJ mol^{-1}.[58] Oxide layers containing Cr are known to reduce corrosion.[59,60] This finding is corroborated by the SEM investigations that reveal more porous

surfaces post dissolution for points with a comparably low Cr content. SEM images of point 6, 8 and 9 appear less affected. A study by Filho *et al.*[61] looked into the effect of alloying elements C, Cr and Nb on wear properties for coatings deposited through high power impulse magnetron sputtering, with 2-fold rotation, and found coatings with a high O content to fail to a larger extent in pin-on-disc set-ups and the cause was believed to be higher reactivity and subsequent dissolution. In contrast to this study the coatings with a high O content did not correlate to coatings with a high Cr content. The possible passivating oxide could reduce the reactivity and hence the dissolution.

ISO standard 10993 recommends 24 h extraction at 37 °C for cytotoxicity.[55] In this study the dissolution was performed for 14 days because a higher concentration of ions was needed for detection with ICP-OES. Consequently a 16 times dilution was necessary to get values of cell viability comparable to the negative control. Indeed, the CoCrMo and SiN controls also showed lower viability for dilutions below 16 times. The

CoCrMo extract showed an adverse effect on the cell viability that could be explained by its high levels of Co ions.[62] The cell viability reduction caused by the SiN extracts could be related to the higher dissolution rate as indicated by the higher levels of Si compared to the alloyed coatings. Previous studies have found that Si promotes proliferation of cells but too high Si concentrations cause cell death.[63] However, the Si concentration that was found to be cytotoxic was 30 times higher than the obtained in the present study. Other negative effects from the dissolution of silicon nitride could be the production of ammonia and high pH.[64,65] However, several studies including indirect cytotoxicity tests of SiN with fibroblasts have shown a good biological response and the results are of course to be interpreted as relative effects rather than absolute ones.[66,67]

Differences in the extraction method could alter the dissolution rate of the material and the cytotoxicity results. However, whereas in the present study the concentration of ions in the extracts was measured, in most of the previous cytotoxicity studies in the literature this data was not included, which makes the comparison more difficult. This was partly mitigated by the inclusion of controls. Since CoCrMo is already used in medical implants, obtaining a higher cell viability with the extracts from the alloyed coatings lends high promise to their further evaluation. Comparing the coatings with a SiN reference coating without alloying elements confirmed the effect of the incorporated elements, namely a reduction of ion release for a greater Cr content in the coating, with an initial increase in cell viability for the extracts from coatings with a higher Cr content up to 5.2%, but a reduction in cell viability for even higher contents. This reduction in viability for lower Cr content in the coating could be explained by the absence of enough Cr to form a protective oxide, leading to a higher ion release. In contrast, a reduction in viability was found for the coatings with Cr content higher than 5.21%, which had a lower ion release. This suggests that the ion release from the coating could be beneficial to the
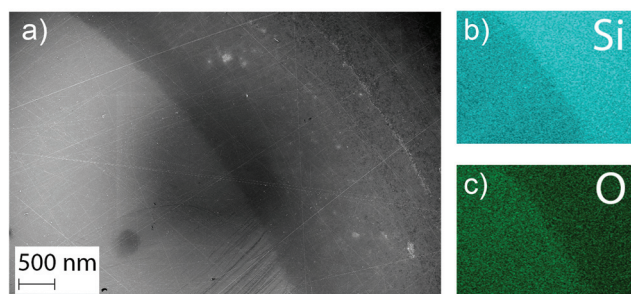

Fig. 9 EDS measurements showing the well in sample 2. (a) shows an SEM image of the border between the dissolved and native area. The EDS measurements revealed a higher Si content (b) in the native area and a higher oxygen (c) content in the part of the sample exposed to cell media.
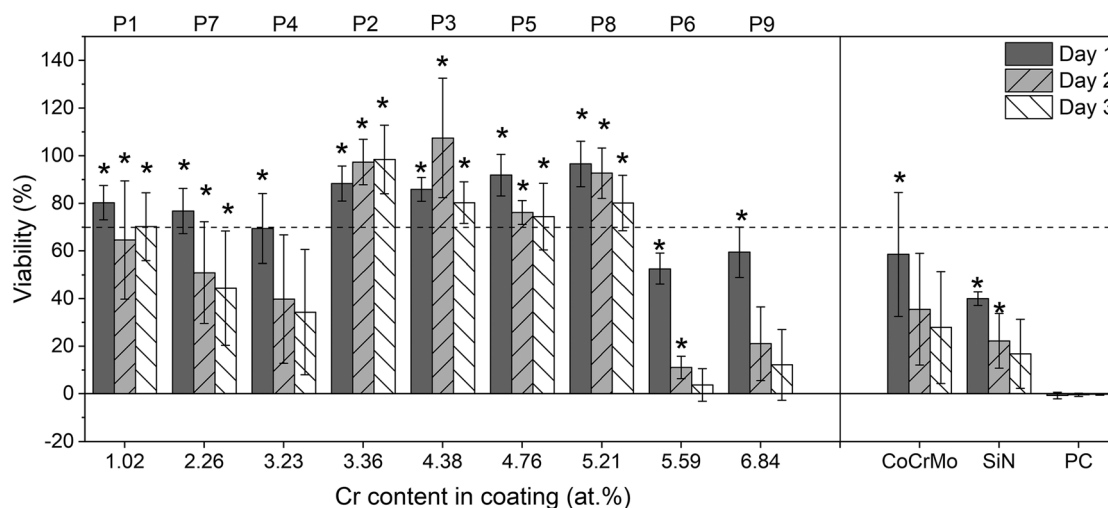

Fig. 10 Cell viability of L929 cells in the presence of the different extracts at 1 : 16 dilution over 3 days. (Mean ± SD; *n* = 9); numbers above the top line stand for the corresponding point of the coating during the deposition. *Significant difference between means (one-way ANOVA plus Dunnett, *p* < 0.05) when compared to the DMSO positive control.

cell response to some extent, possibly supported by the positive effect of Si mentioned above. The Nb release is unlikely to have a major effect, and it has been found not to influence the biocompatibility for TiNbN coatings.[33] However, Li et al.,[68] have reported cytotoxicity for higher ion levels, e.g. 0.172 mg L^{-1}. In the current study, the concentrations of Nb after 4 times dilution are below those cytotoxicity levels reported, i.e. they should not be affecting the results presented. While beyond the scope of this study, this would require further investigation.

Further studies are required before silicon nitride based coatings can be considered an option for biomedical implants. A focus for these studies should be the synergetic effects of wear and corrosion, i.e. tribocorrosion as well as direct cell response studies including immune cells, before moving onto more advanced in vitro and in vivo studies.

Conclusions

This study evaluated silicon nitride-based coatings with the incorporation of Cr and Nb. Overall the coatings had a low surface roughness, high hardness, high elastic modulus and no evident cytotoxicity as compared to CoCrMo and SiN controls, which gave a lower cell viability than the alloyed coatings.

While the adhesion did not seem to be affected by the amount of alloying elements, the use of CrN interlayers improved the adhesion, as expected. The coatings with interlayers showed negligible signs of delamination upon Rockwell indentation, promising for the intended application in medical implants.

The results also showed that silicon nitride-based coatings reduced the ion release from the underlying substrate, as seen by the decrease in Co ion release, regardless of coating composition. The coating composition did however influence the ion release from the coatings themselves and high levels of Cr (between 4.1 at% and 6.0 at%) were found to be beneficial in reducing the overall release of Si, Cr and Nb ions and to the overall dissolution rate of the coating. The cell viability was also influenced by the coating composition and ion release, finding an optimum for Cr contents between 3.2 and 5.3 at%, as a lower ion release initially appeared to lead to an increase in viability, but where the coatings with the lowest ion release caused a reduction in viability, suggesting a certain positive effect on the cell proliferation of some of the ions of the coating. However, to better understand the mechanisms of this phenomena further investigation is required.

Overall, the results are promising as they indicate cytocompatibility as well as a possibility to tailor the dissolution rate of silicon nitride coatings by the use of small amounts of Cr.

Author contributions

Conceptualization, C. S., E. E. and C. P.; methodology, C. S., E. E. and G. H.-B.; investigation, C. S. and E. E.; formal analysis, C. S. and E. E.; data curation, C. S., E. E. and C. P.; writing-original draft preparation, C. S. and E. E.; writing-

review and editing, G. H.-B. and C. P.; supervision, G. H.-B. and C. P.; funding acquisition, C. P. All authors have read and agreed to the published version of the manuscript.

Conflicts of interest

The authors declare no conflict of interest.

Acknowledgements

References

1 Y. Okazaki and E. Gotoh, Metal release from stainless steel, Co-Cr-Mo-Ni-Fe and Ni-Ti alloys in vascular implants, Corros. Sci., 2008, 50(12), 3429–3438, DOI: 10.1016/j.corsci.2008.09.002.

2 T. Hanawa, Metal ion release from metal implants, Mater. Sci. Eng., C, 2004, 24(6–8 SPEC. ISS.), 745–752.

3 L. Savarino, D. Granchi, G. Ciapetti, E. Cenni, A. Nardi Pantoli, R. Rotini, et al., Ion release in patients with metal-on-metal hip bearings in total joint replacement: A comparison with metal-on-polyethylene bearings, J. Biomed. Mater. Res., 2002, 63(5), 467–474.

4 F. S. Haddad, R. R. Thakrar, A. J. Hart, J. A. Skinner, A. V. F. Nargol, J. F. Nolan, et al., Metal-on-metal bearings: The evidence so far, J. Bone Jt. Surg., Br. Vol., 2011, 93(5), 572–579.

5 D. J. Langton, S. S. Jameson, T. J. Joyce, N. J. Hallab, S. Natu and A. V. F. Nargol, Early failure of metal-on-metal bearings in hip resurfacing and large-diameter total hip replacement: A consequence of excess wear, J. Bone Jt. Surg., Br. Vol., 2010, 92(1), 38–46.

6 A. J. Smith, P. Dieppe, P. W. Howard and A. W. Blom, Failure rates of metal-on-metal hip resurfacings: Analysis of data from the National Joint Registry for England and Wales, Lancet, 2012, 380(9855), 1759–1766, DOI: 10.1016/S0140-6736(12)60989-1.

7 G. Grammatopoulos, H. Pandit, Y. M. Kwon, R. Gundle, P. McLardy-Smith, D. J. Beard, et al., Hip resurfacings revised for inflammatory pseudotumour have a poor outcome, J. Bone Jt. Surg., Br. Vol., 2009, 91(8), 1019–1024.

8 Endotec. B-PTM INTEGRATED HIP SYSTEM. Available from: https://www.endotec.com/main/sub01_02_01.php.

9 Implantcast. Knee endoprosthetics.

10 Endotec. B-PTM TOTAL KNEE SYSTEM. Available from: B-PTM INTEGRATED HIP SYSTEM.

11 Corin. AMC MkIITM Mobile Knee System. Available from: https://www.coringroup.com/legacy/medical_professionals/products/knees/amc_mkii/index.html.

12 J. Reich, L. Hovy, H. L. Lindenmaier, R. Zeller, J. Schwiesau, P. Thomas, *et al.*, Präklinische Ergebnisse beschichteter Knieimplantate für Allergiker, *Orthopade*, 2010, **39**(5), 495–502.

13 Aesculap. Aesculap ® Knee Arthroplasty Comparison Smith & Ne.

14 D. H. Park, J. Leong and S. J. Palmer, Total knee arthroplasty with an oxidised zirconium femoral component: a 5-year follow-up study, *J. Orthop. Surg. (Hong Kong)*, 2014, **22**(1), 75–79.

15 M. Innocenti, F. Matassi, C. Carulli, L. Nistri and R. Civinini, Oxidized zirconium femoral component for TKA: A follow-up note of a previous report at a minimum of 10 years, *Knee*, 2014, **21**(4), 858–861, DOI: 10.1016/j.knee.2014.04.005.

16 C. J. Vertullo, P. L. Lewis, S. Graves, L. Kelly, M. Lorimer and P. Myers, *Twelve-Year Outcomes of an Oxinium Total Knee Replacement Compared with the Same Cobalt-Chromium Design*, 2017, pp. 275–283.

17 T. J. Heyse, J. Davis, S. B. Haas, D. X. Chen, T. M. Wright and R. S. Laskin, Retrieval Analysis of Femoral Zirconium Components in Total Knee Arthroplasty. Preliminary Results, *J. Arthroplasty*, 2011, **26**(3), 445–450, DOI: 10.1016/j.arth.2009.11.024.

18 T. J. Heyse, D. X. Chen, N. Kelly, F. Boettner, T. M. Wright and S. B. Haas, Matched-pair total knee arthroplasty retrieval analysis: Oxidized zirconium vs. CoCrMo, *Knee*, 2011, **18**(6), 448–452, DOI: 10.1016/j.knee.2010.08.011.

19 J. K. Hofer and K. A. Ezzet, The Knee A minimum 5-year follow-up of an oxidized zirconium femoral prosthesis used for total knee arthroplasty, *Knee*, 2014, **21**(1), 168–171, DOI: 10.1016/j.knee.2013.08.015.

20 M. Innocenti and R. Civinini, The 5-year Results of an Oxidized Zirconium Femoral Component for TKA, *Clin. Orthop. Relat. Res.*, 2010, 1258–1263.

21 R. W. McCalden, K. D. Charron, R. D. Davidson, M. G. Teeter and D. W. Holdsworth, Damage of an Oxinium femoral head and polyethylene liner following "routine" total hip replacement, *J. Bone Jt. Surg., Br. Vol.*, 2011, **93**(3), 409–413.

22 G. T. Evangelista, E. Fulkerson, F. Kummer and P. E. Di Cesare, Surface damage to an Oxinium femoral head prosthesis after dislocation, *J. Bone Jt. Surg., Br. Vol.*, 2007, **89**(4), 535–537, DOI: 10.1302/0301-620X.89B4.17557.

23 J. Olofsson, M. Pettersson, N. Teuscher, A. Heilmann, K. Larsson, K. Grandfield, *et al.*, Fabrication and evaluation of SixNy coatings for total joint replacements, *J. Mater. Sci. Mater. Med.*, 2012, **23**(8), 1879–1889. Available from: https://www.scopus.com/inward/record.url?eid=2-s2.0-84864917979&partnerID=tZOtx3y1.

24 M. Pettersson, S. Tkachenko, S. Schmidt, T. Berlind, S. Jacobson, L. Hultman, *et al.*, Mechanical and tribological behavior of silicon nitride and silicon carbon nitride coatings for total joint replacements, *J. Mech. Behav. Biomed. Mater.*, 2013, **25**, 41–47. Available from: https://www.sciencedirect.com/science/article/pii/S1751616113001598.

25 M. Ishikawa, K. L. de Mesy Bentley, B. J. McEntire, E. M. Schwarz, C. Xie and B. S. Bal, Surface topography of silicon nitride affects antimicrobial and osseointegrative properties of tibial implants in a murine model, *J. Biomed. Mater. Res., Part A*, 2017, 3413–3421, DOI: 10.1002/jbm.a.36189.

26 G. Pezzotti, R. M. Bock, B. J. Mcentire, E. Jones, M. Bo, W. Zhu, *et al.*, Silicon Nitride Bioceramics Induce Chemically Driven Lysis in Porphyromonas gingivalis, *Langmuir*, 2016, **32**, 3024–3035.

27 F. Boschetto, N. Toyama, S. Horiguchi and R. M. Bock, In vitro antibacterial activity of oxide and non-oxide bioceramics for arthroplastic devices: II.Fourier transform infrared spectroscopy, *Analyst*, 2018, 2128–2140.

28 E. Laarz, B. V. Zhmud and L. Bergström, Dissolution and Deagglomeration of Silicon Nitride in Aqueous Medium, *J. Am. Ceram. Soc.*, 2004, **83**(10), 2394–2400, DOI: 10.1111/j.1151-2916.2000.tb01567.x.

29 B. V. Zhmud and L. Bergström, Dissolution Kinetics of Silicon Nitride in Aqueous Suspension, *J. Colloid Interface Sci.*, 1999, **218**(2), 582–584. Available from: https://www.sciencedirect.com/science/article/pii/S0021979799964251.

30 M. Pettersson, C. Skjöldebrand, L. Filho, H. Engqvist and C. Persson, Morphology and Dissolution Rate of Wear Debris from Silicon Nitride Coatings, *ACS Biomater. Sci. Eng.*, 2016, **2**(6), 998–1004.

31 M. Pettersson, M. Bryant, S. Schmidt, H. Engqvist, R. M. Hall, A. Neville, *et al.*, Dissolution behaviour of silicon nitride coatings for joint replacements, *Mater. Sci. Eng., C*, 2016, **62**, 497–505. Available from: https://www.scopus.com/inward/record.url?eid=2-s2.0-84957553843&partnerID=tZOtx3y1.

32 L. C. Filho, S. Schmidt, A. López, M. Cogrel, K. Leifer, H. Engqvist, *et al.*, The effect of coating density on functional properties of SiNx coated implants, *Materials*, 2019, **12**(20), 11–14.

33 V. Ragone, E. Canciani, C. A. Biffi, R. D'Ambrosi, R. Sanvito and C. Dellavia, CoCrMo alloys ions release behavior by TiNbN coating: an *in vitro* study, *Biomed. Microdevices*, 2019, **21**(3), 61.

34 E. Thienpont, Titanium niobium nitride knee implants are not inferior to chrome cobalt components for primary total knee arthroplasty, *Arch. Orthop. Trauma. Surg.*, 2015, **135**(12), 1749–1754.

35 ISO 5832-4:2014. Implants for surgery - Metallic materials - Part 4: Cobalt-chromium-molybdenum casting alloy. 2014. Available from: https://www.iso.org/ics/11.040.40/x/.

36 A. Frisk, F. Magnus, S. George, U. B. Arnalds and G. Andersson, Tailoring anisotropy and domain structure in amorphous TbCo thin films through combinatorial methods, *J. Phys. D: Appl. Phys.*, 2016, **49**(3), 035005. Available from: https://www.scopus.com/inward/record.url?eid=2-s2.0-84954172750&partnerID=tZOtx3y1.

37 J. J. Vlassak and W. D. Nix, Measuring the Elastic Properties of Materials By Means of Indentation, *J. Mech. Phys. Solids*, 1994, **42**(8), 1223–1245.

38 ISO 26443. Internation Standard: Fine ceramics (advanced ceramics, advanced technical ceramics) – Rockwell indentation test for evaluation of adhesion of ceramic coatings. 2008.

39 T. Abubakar, M. Rahman, D. P. Dowling, J. Stokes and M. S. J. Hashmi, Adhesion performance of TiN coating with amorphous NiTi alloy interlayer onto 316L stainless biosteel deposited by sputtering process, *Surf. Eng.*, 2010, **26**(7), 499–505.

40 I. Endler, A. Leonhardt, H. J. Scheibe and R. Born, Interlayers for diamond deposition on tool materials, *Diamond Relat. Mater.*, 1996, **5**(3–5), 299–303.

41 J. Gerth and U. Wiklund, The influence of metallic interlayers on the adhesion of PVD TiN coatings on high-speed steel, *Wear*, 2008, **264**(9–10), 885–892.

42 H. K. Kim, J. H. La, K. S. Kim and S. Y. Lee, The effects of the H/E ratio of various Cr-N interlayers on the adhesion strength of CrZrN coatings on tungsten carbide substrates, *Surf. Coat. Technol.*, 2015, **284**, 230–234, DOI: 10.1016/j.surfcoat.2015.06.077.

43 J. Tang, L. Feng and J. S. Zabinski, The effects of metal interlayer insertion on the friction, wear and adhesion of TiC coatings, *Surf. Coat. Technol.*, 1998, **99**(3), 242–247.

44 C. A. Davis, A simple model for the formation of compressive stress in thin films by ion bombardment, *Thin Solid Films*, 1993, **226**(1), 30–34.

45 S. Schmidt, T. Hänninen, C. Goyenola, J. Wissting, J. Jensen, L. Hultman, *et al.*, SiNx Coatings Deposited by Reactive High Power Impulse Magnetron Sputtering: Process Parameters Influencing the Nitrogen Content, *ACS Appl. Mater. Interfaces*, 2016, **8**(31), 20385–20395.

46 C. Skjöldebrand, G. Hulsart-Billström, H. Engqvist and C. Persson, Si-Fe-C-N coatings for biomedical applications: A combinatorial approach, *Materials*, 2020, **13**(9), 1–16.

47 C. Skjöldebrand, S. Schmidt, V. Vuong, M. Pettersson, K. Grandfield, H. Högberg, *et al.*, Influence of substrate heating and nitrogen flow on the composition, morphological and mechanical properties of SiNx coatings aimed for joint replacements, *Materials*, 2017, **10**(2), 1–11.

48 ISO 7206-2. Implants for surgery—Partial and total hip joint prostheses—Part 2: Articulating surfaces made of metallic, ceramic and plastics materials. 2018; .

49 M. Čekada, P. Panjan, D. Kek-Merl, M. Panjan and G. Kapun, SEM study of defects in PVD hard coatings, *Vacuum*, 2007, **82**(2), 252–256. Available from: https://www.sciencedirect.com/science/article/pii/S0042207X07002151.

50 M. Meissner, T. Tolg, P. Baroch and J. Musil, Elimination of arcing in reactive sputtering of Al2O3 thin films prepared by DC pulse single magnetron, *Plasma Processes Polym.*, 2011, **8**(6), 500–504.

51 A. Belkind, A. Freilich and R. Scholl, Using pulsed direct current power for reactive sputtering of Al2O3, *J. Vac. Sci. Technol., A*, 1999, **17**(4), 1934–1940.

52 L. Fu, Y. Xiong, G. Carlsson, M. Palmer, S. Örn, W. Zhu, *et al.*, Biodegradable Si3N4 bioceramic sintered with Sr, Mg and Si for spinal fusion: Surface characterization and biological evaluation, *Appl. Mater. Today*, 2018, **12**, 260–275.

53 L. Fu, H. Engqvist and W. Xia, Spark plasma sintering of biodegradable Si3N4 bioceramic with Sr, Mg and Si as sintering additives for spinal fusion, *J. Eur. Ceram. Soc.*, 2018, **38**(4), 2110–2119.

54 Standardization IO for ISO 10993-12 Biological evaluation of medical devices. ISO 10993-12, 2012.

55 Standardization IO for ISO 10993-5 Biological evaluation of medical devices. 61010-1©Iec2001. 2006, 2006, 13.

56 X. Liu, T. Xi and Y. Zheng, Influence of the extraction parameters on the cytotoxicity test results of Mg materials, *Prog. Nat. Sci.: Mater. Int.*, 2014, **24**(5), 507–515.

57 E. Jablonská, J. Kubásek, D. Vojtěch, T. Ruml and J. Lipov, Test conditions can significantly affect the results of in vitro cytotoxicity testing of degradable metallic biomaterials, *Sci. Rep.*, 2021, **11**(1), 1–9.

58 CRC. Handbook of Chemistry and Physics Online. [cited 2021 Dec 13]. Available from: https://hbcp.chemnetbase.com/faces/contents/InteractiveTable.xhtml.

59 I. Olefjord, Esca-studies of the composition profile of low temperature oxide formed on chromium steels-I. Oxydation in dry oxygen, *Corros. Sci.*, 1975, **15**(6–12), 687–696.

60 R. I. M. Asri, W. S. W. Harun, M. Samykano, N. A. C. Lah, S. A. C. Ghani, F. Tarlochan, *et al.*, Corrosion and surface modification on biocompatible metals: A review, *Mater. Sci. Eng., C*, 2017, **77**, 1261–1274, DOI: 10.1016/j.msec.2017.04.102.

61 L. C. Filho, S. Schmidt, C. Goyenola, C. Skjöldebrand, H. Engqvist, H. Högberg, M. Tobler and C. Persson, The effect of N, C, Cr, and Nb content on silicon nitride coatings for joint applications, *Materials*, 2020, **13**(8), 1896.

62 L. J. Smith, A. L. Holmes, S. K. Kandpal, M. D. Mason, T. Zheng and J. P. Wise, The cytotoxicity and genotoxicity of soluble and particulate cobalt in human lung fibroblast cells, *Toxicol. Appl. Pharmacol.*, 2014, **278**(3), 259–265.

63 M. Y. Shie, S. J. Ding and H. C. Chang, The role of silicon in osteoblast-like cell proliferation and apoptosis, *Acta Biomater.*, 2011, **7**(6), 2604–2614.

64 G. Pezzotti, R. M. Bock, T. Adachi, A. Rondinella, F. Boschetto, W. Zhu, *et al.*, Silicon nitride surface chemistry: A potent regulator of mesenchymal progenitor cell activity in bone formation, *Appl. Mater. Today*, 2017, **9**, 82–95.

65 G. Pezzotti, Silicon Nitride: A Bioceramic with a Gift, *ACS Appl. Mater. Interfaces*, 2019, **11**(30), 26619–26636.

66 M. Mazzocchi and A. Bellosi, On the possibility of silicon nitride as a ceramic for structural orthopaedic implants. Part I: Processing, microstructure, mechanical properties, cytotoxicity, *J. Mater. Sci.: Mater. Med.*, 2008, **19**(8), 2881–2887.

67 M. Hnatko, M. Hičák, M. Labudová, D. Galusková, J. Sedláček, Z. Lenčéš, *et al.*, Bioactive silicon nitride by surface thermal treatment, *J. Eur. Ceram. Soc.*, 2020, **40**(5), 1848–1858, DOI: 10.1016/j.jeurceramsoc.2019.12.053.

68 Y. Li, C. Wong, J. Xiong, P. Hodgson and C. Wen, Cytotoxicity of titanium and titanium alloying elements, *J. Dent. Res.*, 2010, **89**(5), 493–497.